Radiated Susceptibility Analysis of Multiconductor Transmission Lines Based on Polynomial Chaos

Tianhao Wang [1], Quanyi Yu [1], Xianli Yu [2], Le Gao [1], and Huanyu Zhao [1*]

[1] College of Instrumentation and Electrical Engineering
Jilin University, Changchun, 220000, 130061 China
wangtianhao@jlu.edu.cn, yqy17@mails.jlu.edu.cn, gaole@jlu.edu.cn, zhaohyjlu@jlu.edu.cn*

[2] College of Geo-Exploration Science and Technology
Jilin University, Changchun, 220000, 130061 China
yuxianli@jlu.edu.cn

Abstract **–** To address the uncertainties of the radiated susceptibility of multiconductor transmission lines (MTLs), a surrogate model of the MTLs radiated susceptibility is established based on generalized polynomial chaos (gPC), and the gPC is made sparser by combining the adaptive hyperbolic truncation (AHT) scheme and the least angle regression (LAR) method. The uncertainties of the radiated susceptibility of transmission lines are calculated using the adaptive-sparse polynomial chaos (AS-PC) scheme. The parameters related to the incident field, such as elevation angle θ, azimuth angle ψ, polarization angle η, and field amplitude E, are inevitably random. Therefore, these four variables are taken as random input variables, and each of them is subject to different variable distributions. The MTLs model with infinite ground as the reference conductor is adopted, different impedances are used and the AS-PC scheme is combined with transmission line theory to calculate the average, standard deviation and probability distribution of the radiated susceptibility of MTLs. Sobol global sensitivity analysis based on variance decomposition is adopted to calculate the influence of random input variables on the MTLs radiated susceptibility model. The calculation results are compared with the results of the Monte Carlo (MC) method, proving that the proposed method is correct and feasible.

Index Terms **–** Adaptive Hyperbolic Truncation (AHT), Least Angle Regression (LAR), Multiconductor Transmission Lines (MTLs), polynomial chaos, radiated susceptibility.

I. INTRODUCTION

The electromagnetic compatibility problem caused by the complex electromagnetic environment has attracted more and more attention of researchers. Transmission lines, as the carrier of power and signal, are an indispensable part of electrical and electronic equipment. As an important problem in electromagnetic compatibility, MTLs radiated susceptibility has received increasing research attention. By combining the transmission line equation, the solution of the double-conductor transmission lines radiated susceptibility equation is obtained when the relevant parameters of the incident field are determined [1]. Then, the double-conductor transmission line model is extended to a more complex MTLs model, and the frequency-domain response of the radiated susceptibility of MTLs is obtained by [2,3].

Due to the complexity of the electromagnetic environment and the possible position change of the electronic equipment, the relevant parameters of the incident field (such as elevation angle θ, azimuth angle ψ, polarization angle η, and field amplitude E) will inevitably have uncertainties. In the past decades, the uncertainties of transmission line radiated susceptibility have been studied. Researches used stochastic reduced-order models to analyze the uncertainties of induced current generated by MTLs radiated by random plane wave [4]. The probability immunity method was used to analyze the radiated susceptibility of a double-conductor electric short transmission line incident by a random plane wave [5], and the statistical characteristics of the response current of MTLs excited by a random plane wave were analyzed [6]. [7] studied the simulations of uniform and non-uniform transmission lines and compared the results of the two. The time domain model of MTLs in the ordinary differential equation form was used in reference [8] to analyze the fast response of MTLs in the field line coupling situation, and the BLT (Beam-Liu-Tesche) equation [9] was used to calculate the frequency-domain response of lossless MTLs under plane wave radiation. A PCB radiated electromagnetic compatibility model [10] is established, which can accurately reproduce the NFS signals emitted by electronic circuits with transient excitation of nanoseconds duration. For the uncertainties of electromagnetic coupling of

Submitted On: May 4, 2020
Accepted On: August 9, 2020

https://doi.org/10.47037/2020.ACES.J.351215

MTLs, the probability distribution model of the electromagnetic coupling of MTLs is established by combining the full-factor numerical integration, sparse-grid numerical integration, and maximum entropy methods [11]. Polynomial chaos [12] was used to analyze the uncertainties of the electromagnetic coupling of a naval ship harness. Similarly, [13-15] combined with the gPC analyzed the uncertainties of radiated susceptibility. In order to predict the model more efficiently, least angle regression method [16] is proposed, and on this basis, a sparse chaos polynomial is proposed [17], which is used to solve the engineering probability problem. In view of different transmission line types, the frequency-domain response of the twisted pair transmission lines radiated susceptibility with ground as the reference conductor was analyzed [18]. Analogously, the twisted pair transmission lines radiated susceptibility model [19] was established by using the variable distance function and the moment method. The uncertainties of the radiated susceptibility of the randomly wound transmission line model with ground as the reference conductor was calculated and analyzed [20].

Quantify the uncertainties of the model output is at the heart of uncertainty analysis. Therefore, global sensitivity analysis which can quantitatively analyze the impact of the interaction between multiple input variables on the model outputs is necessary. The global sensitivity analysis method mainly includes the Sobol method based on variance decomposition [21]. First-and second-order reliability methods are used to analyze the reliability and global sensitivity of the radiated susceptibility of MTLs [22].

On the basis of the gPC, this paper proposes an AS-PC method that combines the AHT scheme with the LAR to analyze the uncertainties of the radiated susceptibility of MTLs with different impedances and combines it with the Sobol global sensitivity analysis method based on variance decomposition to calculate the global sensitivity of the input variables of the radiated susceptibility of MTLs. Finally, the total and first-order sensitivity indices are obtained, and the influence degree of different input variables on the transmission line radiated susceptibility model is analyzed quantitatively. The calculation results are compared with the results of 20000 MC realizations to verify the correctness and efficiency of this method.

II. ADAPTIVE SPARSE POLYNOMIAL CHAOS

The polynomial chaos from the homogeneous function [23,24] in Wiener theory has a solid mathematical foundation and can accurately describe the randomness of variables in any form of distribution. Wiener first used Hermite orthogonal polynomials based on Gaussian random variables to establish polynomial chaos. Later, Xu and Karniadakis extended them to more traditional random variable distribution types through the Askey scheme and obtained a gPC with a wider range of application [25]. The orthogonal polynomials corresponding to the distribution types of the traditional random input variables are shown in Table 1.

Let the original model be $Y = y(\xi)$ and expand it with the gPC scheme. The result is as follows:

$$\begin{aligned} Y &= c_0 I_0 + \sum_{i_1=1}^{\infty} c_{i_1} I_1\left(\xi_{i_1}\right) + \sum_{i_1=1}^{\infty}\sum_{i_2=1}^{i_1} c_{i_1 i_2} I_2\left(\xi_{i_1},\xi_{i_2}\right) + \\ &\quad \sum_{i_1=1}^{\infty}\sum_{i_2=1}^{i_1}\sum_{i_3=1}^{i_2} c_{i_1 i_2 i_3} I_3\left(\xi_{i_1},\xi_{i_2},\xi_{i_3}\right) + \cdots \\ &= \sum_{i=0}^{\infty} \hat{c}_i \Phi_i\left(\boldsymbol{\xi}\right). \end{aligned} \tag{1}$$

Table 1: Orthogonal polynomials corresponding to distribution types

Distribution Type	Probability Density Function	Orthogonal Polynomial	Weight Function	Variable Range
Normal	$\frac{1}{\sqrt{2\pi}} e^{-x^2/2}$	Hermite $H_n(x)$	$e^{-x^2/2}$	$[-\infty,+\infty]$
uniform	$\frac{1}{\sqrt{2\pi}} e^{-x^2/2}$ 1/2	Legendre $P_n(x)$	1	[-1,1]
β	$\frac{(1-x)^{\alpha}(1+x)\beta}{2^{\alpha+\beta+1}B(\alpha+1,\beta+1)} e^{-x}$	Jacobi $P_n^{(\alpha,\beta)}(x)$	$(1-x)^{\alpha}(1+x)\beta$	[-1,1]
exponential	e^{-x}	Laguerre $L_n(x)$	e^{-x}	$[0,+\infty]$

In (1), $I_n\left(\xi_{i_1},\cdots,\xi_{i_n}\right)$ represents a mixed orthogonal polynomial of *n* order, which is a function of multi-dimensional standard random variables $\left[\xi_{i_1},\cdots,\xi_{i_n}\right]$. $\hat{c}_i$ and Φ_i correspond to $c_{i_1 i_2 \cdots i_p}$ and $I_n\left(\xi_{i_1},\ldots,\xi_{i_n}\right)$ in (1), respectively. Polynomial chaos expansion $\Phi_i(\boldsymbol{\xi})$ is the product of the one-dimensional orthogonal polynomial basis function corresponding to each random variable. The number of terms in the expansion of gPC is theoretically infinite. To calculate the coefficients of the

gPC expansion, the traditional method must select the highest order P of the polynomial and truncate it at the P order, and the obtained polynomial chaos expansion is:

$$Y = \sum_{i=0}^{P} \hat{c}_i \Phi_i(\boldsymbol{\xi}). \tag{2}$$

When the dimension of the input variables of the model is n, the number of truncated polynomial chaos expansion terms (N) is:

$$N = \frac{(P+n)!}{P!n!}. \tag{3}$$

One of the core functions of the gPC method is solving the expansion term coefficient ($\hat{c}_i$), which is generally calculated by the regression or projection method. (3) indicates that the number of terms of the expansion increases with the dimension of the input variables and the truncation order of the gPC scheme, resulting in a dimension problem and reducing the coefficient calculation efficiency of the expansion term of the gPC scheme. If the truncation order is reduced, then the solution accuracy of the expansion coefficient cannot be guaranteed. Therefore, the key to solving the problem is to use an appropriate truncation method and the sparse method to reduce the polynomial, which is not very important in the expansion term of gPC.

A. Adaptive hyperbolic truncation

According to the effect sparsity and ordering principles of the model [26], the lower-order effect in the model is more important than the higher-order effect, and focus should be on the "important few" rather than the "unimportant many." The hyperbolic truncation scheme can effectively reduce the high-order effect factors among the variables in the model [27]. Let p_i be the highest order of Φ_i, and the order of the k-th dimension random variable is l_k when the traditional truncation scheme is adopted:

$$p_i = \sum_{k=1}^{n} l_k = l_1 + l_2 + \cdots + l_n. \tag{4}$$

Given that the concept of norm is used in the hyperbolic truncation scheme, and q refers to the norm, then (4) is redefined as:

$$p_i = \left(\sum_{k=1}^{n} (l_k)^q \right)^{1/q} \le P, 0 < q \le 1. \tag{5}$$

(5) shows that when q = 1, $P_{\max} = P$, the truncation scheme is the traditional truncation scheme. Meanwhile, the hyperbolic truncation scheme parses the high-order effect of the model on the basis of the traditional truncation scheme. When q <1, all the remaining polynomials are located under the hyperbolic curve or surface. To intuitively show the truncation effect of the hyperbola, two-dimensional input variables are taken as examples, as shown in Fig. 1.

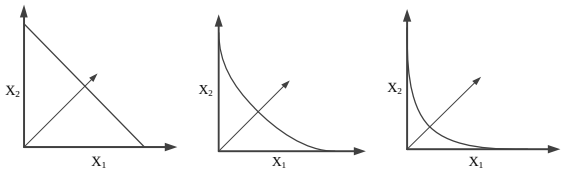

n=2, *q*=1 *n*=2, *q*=0.75 *n*=2, *q*=0.5

Fig. 1. Hyperbolic truncation diagram of different dimension input variables and q norms.

Figure 1 shows that for input variables of different dimensions, the hyperbolic truncation scheme can effectively reduce the high-order effect of the model and maintain the low-order effect below the curve. In Fig. 1, when q = 1, the hyperbola is a straight line, as shown in a; when q < 1, the straight line becomes a hyperbola, as shown in b and c. With the decrease of q, the penalty of the hyperbolic truncation scheme for the high-order effect of the model is more obvious. The traditional truncation order (P = 5) and the input variable dimension (n = 2) are taken as examples, as shown in Fig. 2.

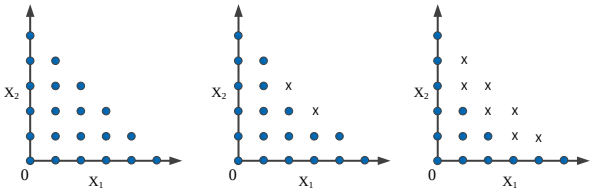

P=5, *q*=1 *P*=5, *q*=0.75 *P*=5, *q*=0.5

Fig. 2. Truncation effect of hyperbolic truncation when P=5, n = 2.

To show the influence of the related sparse processing method on the model, let g be the sparse coefficient:

$$g = N'/N. \tag{6}$$

In the above equation, N' is the number of polynomial expansion terms after sparse processing, and N is the number of polynomial expansion terms without sparse processing. For the model with n = 4 (input variables) and q = 0.8 (hyperbolic truncation norm), the sparse coefficients generated by different truncations are shown in Table 2.

Table 2: Comparison of the number of polynomial terms of the traditional and hyperbolic truncation schemes with different truncation orders

	Traditional	q=0.8	*g*
P=5	126	61	48.4%
P=10	1001	408	40.8%
P=15	3876	1476	38.1%

Table 2 shows that the hyperbolic truncation scheme can effectively reduce the number of polynomial terms, and the sparse coefficients decrease with the increase in the truncation order. Thus, the hyperbolic truncation scheme can effectively perform the preliminary sparse processing of the model. In practical calculation and analysis, the choice of hyperbolic truncation norm q is important. When the value of norm q is extremely low, although many high-order effects are removed, the low-order effects of the model are also affected, resulting in an extremely large error in the final calculation results of the model. In view of the selection of the hyperbolic truncation norm q, an adaptive method is proposed to select the appropriate hyperbolic truncation norm q, which takes the leave-one-out (*LOO*)verification error as the criterion.

The LOO cross-validation error uses cross-validation to overcome the overfitting problem caused by the normalized empirical error, which is a technology developed in statistical learning. Let the *LOO* cross-validation error be ε_{LOO}. m metamodels are established, with each based on the simplified experimental design, and their predictions are compared at the exclusion point with the true value ε_{LOO} can be expressed as follows:

$$\varepsilon_{LOO} = \frac{\sum_{i=1}^{m}\left(M\left(x^{(i)}\right) - M^{PC\backslash i}\left(x^{(i)}\right)\right)^2}{\sum_{i=1}^{N}\left(M\left(x^{(i)}\right) - \hat{\mu}Y\right)^2}. \tag{7}$$

In (7), $M(x^{(i)})$ is the response value of the model at point $x^{(i)}$ of the ith metamodel, $M^{PC\backslash i}(x^{(i)})$ is the response value of the polynomial chaos model at point $x^{(i)}$ of the ith metamodel, and $\hat{\mu}$ is the mean value.

The main steps of the selection algorithm of AHT norm q with ε_{LOO} as the criterion are as follows:

(1) Set the selection range of hyperbolic truncation norm q to [a, b] and the step size to s.
(2) Set threshold of ε_{LOO}.
(3) When ε_{LOO} is less than the set threshold or exceeds the maximum selection range, the program stops, and the obtained g value is the final selection result.

B. Least angle regression

The AHT can effectively reduce the influence of high-order effects among variables in the model. Table 2 shows that although the number of polynomial terms after hyperbolic truncation is reduced by more than half compared with the traditional gPC, some space remains for the sparse processing of the number of polynomial terms after the AHT due to the large number of basic terms of the polynomials. LAR is an important sparse algorithm that can effectively make the model sparser. Therefore, on the basis of the AHT, LAR is used to sparse the hyperbolic truncation polynomials to further sparse the number of terms of the polynomial chaos. In 2004, Efron proposed a variable selection method similar to forward stepwise regression [16]. The main idea of LAR is as follows:

The model is represented as $Y = X\theta$, using the cosine similarity method to select the most relevant independent variable (X_j) with dependent variable Y. The residual (γ) of Y and X_j is calculated, moving in the direction of X_j until another variable X_t appears. The correlation between X_t and residual γ is equal to that between X_j and residual γ, that is, residual γ is located on the angle bisector of X_j and X_t and then continues to move forward along the angle bisector until the next independent variable that is most related to the residual appears. In short, we are constantly looking for variables that are most relevant to the current residual. Taking the two-dimensional input variables as an example, the schematic of LAR is shown in Fig. 3. The main steps of LAR are as follows:

(1) Let all polynomial coefficients be 0, and the initial residual γ be the observation vector.
(2) Find the most relevant variable (X_1) with dependent variable Y by cosine similarity.
(3) Let variable X_1 move in the current direction until X_1 and X_2 can be divided equally, that is, until the correlation between X_2 and the residual is the same as that between X_1 and residual γ. At this time, residual γ is located on the angular bisector of X_1 and X_2.
(4) Similar to Step 2, continue to move in the direction of the angular bisector obtained in Step 2 until a new independent variable (X_3) appears with the same degree of correlation as residual γ.
(5) Update the coefficients and move eligible arguments from the candidate set to the active set.
(6) Repeat the above steps until all variables are iterated.

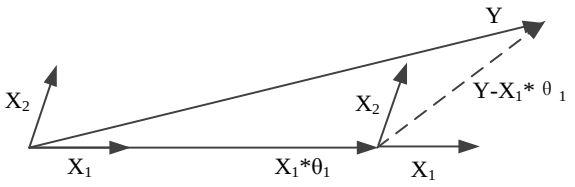

Fig. 3. LAR of two-dimensional input variables.

C. Global sensitivity analysis based on polynomial chaos

The Sobol method is the most classical among the global sensitivity analysis methods. In this method, the interaction between single and multiple input variables is ANOVA, and their contribution to the model output variance is calculated to analyze the influence degree of different single or multiple variables' interaction on the

output model, that is, the idea of ANOVA. With the use of the Sobol method, the output model is decomposed into the sum of 2^n increasing terms:

$$Y(\boldsymbol{\xi}) = y_0 + \sum_{i=1}^{n} y_i(\xi_i) + \sum_{1\le i\le j\le n} y_{ij}(\xi_i,\xi_j) + y_{1,2,\ldots,n}(\xi_1,\xi_2,\ldots,\xi_n). \quad (8)$$

In (8), ξ represents the *n*-dimensional input variables [ξ_1, ξ_2, …, ξ_n], y_0 is the mean value of Y (ξ), and the decomposition terms have an orthogonal relationship. The coefficients of each decomposition term in (8) can be obtained by recursively calculating the sum of the expansion terms through an integral. To obtain the variance decomposition formula, the variance is taken from both sides of (8):

$$Var\left[Y(\xi)\right] = D = \sum_{i=1}^{n} D_i + \sum_{1\le i< j\le n} D_{ij} + \cdots + D_{1,2,\ldots,n} \quad (9)$$

The different decomposition terms in (9) represent the influence of different input variables and the interaction between variables on the output response variance. The Sobol sensitivity indices are defined as:

$$S_{i_1,\ldots,i_s} = \frac{D_{i_1,\ldots,i_s}}{D}, 1\le i_1<\ldots<i_s\le n; s=1,\ldots,n. \quad (10)$$

S_i refers to the first-order sensitivity indices, which represent the contribution of a single input to the output response variance. The sum of the first-order sensitivity indices of each input variable and the sensitivity indices of the interaction between each variable is defined as the total sensitivity indices

$$S_i^T = S_i + \sum_{j<i} S_{j,k,i} + \cdots + S_{1,2,\cdots,n}. \quad (11)$$

In the early days of the Sobol method, the total sensitivity indices and the sensitivity indices of each order were calculated by MC. However, MC has a high calculation cost and a low calculation efficiency. Therefore, this paper combines AS-PC and the Sobol method to calculate the total sensitivity indices and the sensitivity indices of each order [28]:

$$Y(\xi) = c_0 + \sum_{i=1}^{n}\sum_{\alpha\in I_i} c_\alpha\Phi_\alpha(\xi_\alpha) + \sum_{1\le i_1<i_2\le n}\sum_{\alpha\in I_{i_1,i_2}} c_\alpha\Phi_\alpha(\xi_{i_1},\xi_{i_2}) + \cdots + \sum_{1\le i_1<\cdots<n}\sum_{\alpha\in I_{i_1,\cdots,i_s}} c_\alpha\Phi_\alpha(\xi_{i_1},\cdots,\xi_{i_s}) + \sum_{\alpha\in I_{1,\ldots,n}} c_\alpha\Phi_\alpha(\xi_1,\cdots,\xi_n). \quad (12)$$

In (12),

$$I_{i_1,\ldots,i_s} = \left\{\begin{matrix}\alpha\in(\alpha_1,\alpha_2,\cdots,\alpha_n):\alpha_k=0;\\ k\notin(i_1,\cdots,i_s),\forall k=1,\cdots,n\end{matrix}\right\}. \quad (13)$$

$Y(\xi)$ can be calculated:

$$Y(\xi) = \sum_{\alpha\in I_{i_1,\cdots,i_s}} c_\alpha\Phi_\alpha(\xi_{i_1},\ldots,\xi_{i_s}). \quad (14)$$

According to the orthogonality of the basis functions of polynomial chaos,

$$D_{i_1,\ldots,i_s} = \sum_{\alpha\in I_{i_1,\cdots,i_s}} c_\alpha^2. \quad (15)$$

The global sensitivity indices of Sobol based on AS-PC, including the first-order and total sensitivity indices, can be obtained by combining (10) and (11).

III. NUMERICAL EXAMPLE

This paper focuses on the research and analysis of the uniform lossless MTLs with ground as the reference conductor. In real life, all kinds of electrical and electronic equipment and large-scale systems are exposed to complex electromagnetic environment, and the uncertainty factors that lead to the electromagnetic compatibility radiated susceptibility of transmission lines in all kinds of equipment and systems are mainly concentrated in the incident field generated by the external electromagnetic environment. The elevation angle (θ), azimuth angle (ψ), polarization angle (η), and level amplitude (E) of the incident plane wave of the MTLs system with the ground as the reference conductor is shown in Fig. 4.

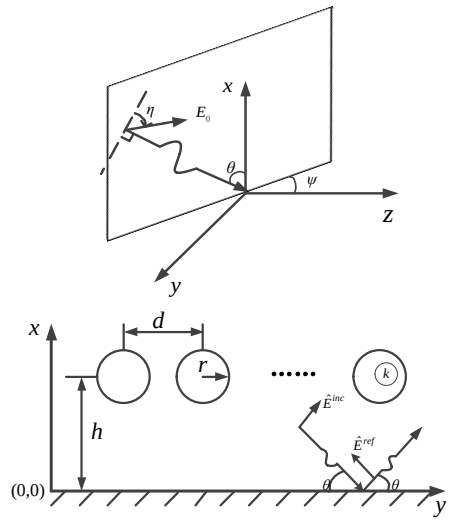

Fig. 4. Relationship between plane incident wave and transmission line position.

Where *d* is the distance between transmission lines, *h* is the height of the transmission lines from the ground,

r is the radius of the transmission lines, θ is the elevation angle, ψ is the azimuth angle, η is the polarization angle and E_0 is the level amplitude of the incident plane wave.

In this section, the gPC model of the radiated susceptibility of MTLs is established. The random input variables of MTLs radiated susceptibility are θ, ψ, η, and the E_0. According to the distribution type of each variable, the corresponding orthogonal substrate can be determined and the gPC proxy model can be established.

The number of transmission lines is 3, and a (3+1) MTLs model with the ground as the reference conductor is established. As shown in Fig. 5, the length of the transmission lines is l = 1m, the radius is r = 0.4mm, the distance between transmission lines is 1cm, the height (h) from the ground is 2cm. The impedance of the source end and the load end of the transmission line are set as low impedance and high impedance respectively. The radiated susceptibility under different impedance conditions is compared and analyzed.

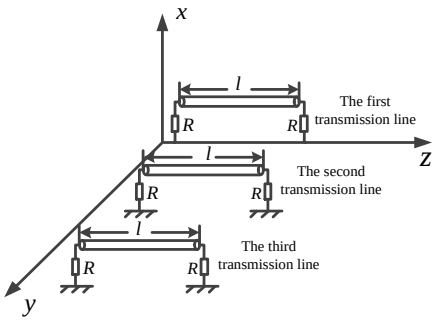

Fig. 5. (3+1) MTLs system.

The random input variables in the example are the elevation angle (θ), azimuth angle (ψ), polarization angle (η), and level amplitude (E) of the incident plane wave. Elevation angle θ is subject to uniform distribution on the interval [0,0.5π], azimuth angle ψ is subject to uniform distribution on the interval [- π, π], polarization angle η is subject to uniform distribution on the interval [0,2π], and level amplitude E is subject to normal distribution with a mean value of 1 V/M and a standard deviation of 0.2v/m. According to the different distributions of random input variables, the corresponding orthogonal basis is selected to build the gPC model. In the traditional truncation scheme, taking the remote induced current (I_{R2}) of the second transmission line in Fig. 5 as an example, truncation orders (P) 5, 10, 15, and 20 are used. In the case of low impedance and high impedance respectively, the mean value and standard deviation of the gPC model of MTLs radiated susceptibility are calculated, the low impedance is 50Ω, and the high impedance is 10kΩ. The frequency range of the incident field is set to [10MHz, 1GHz], and the calculated mean value and the standard deviation are combined with the calculation of 20000 MC runs. The results are shown in Fig. 6.

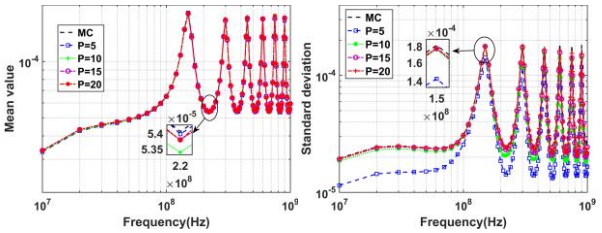

(a) Comparison of mean value and standard deviation of low impedance

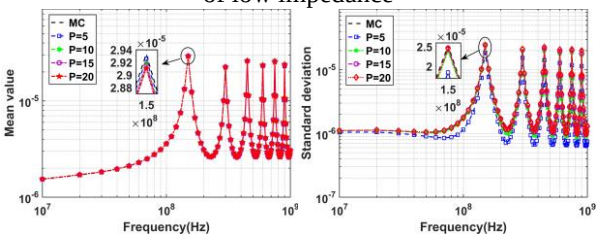

(b) Comparison of mean value and standard deviation of high impedance

Fig. 6. Comparison between the mean value and standard deviation of traditional gPC with different truncation orders and the 20000 MC realizations.

According to the comparison results in Fig. 6, for the mean value and standard deviation of the radiated susceptibility induced current (I_{R2}) of the MTLs, the calculation results of the standard deviation of the low-order truncation are poor under the traditional truncation scheme, but the calculation results of the mean value and standard deviation approach the calculation results of MC as the truncation order increased. Next, for different truncation orders (P), we select ε_{LOO} at three frequency points (i.e., 50, 80, and 100MHz) for comparison, as shown in Fig. 7. Figure 7 shows that the lower-order truncation, such as the 5th and 10th order truncations, is relatively large, and the calculation results are not ideal, whereas the ε_{LOO} of the 15th and the 20th order truncations are relatively low and basically consistent. Therefore, the calculation accuracy increases with the truncation order (P), indicating that the 15th-order truncation can achieve a high accuracy in the traditional truncation.

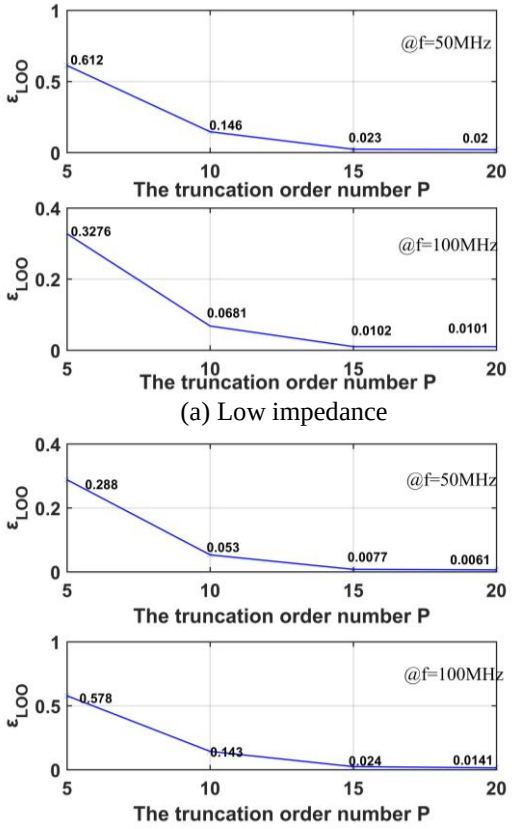

(a) Low impedance

(b) High impedance

Fig. 7. ε_{LOO} comparison between different frequency points and different truncation order.

According to (3), 3876 expansions of gPC exist in the traditional truncation scheme of order 15.A large sparse processing space remains in gPC. To further reduce the calculation cost and improve the calculation efficiency, the AHT scheme introduced earlier is used to deal with the polynomials. Taking the induced current (I_{R2}) at 50MHz as an example, the selection interval of hyperbolic truncation norm q is [0.5,1], the step s is 0.05, and the threshold value is 0.05. It is also calculated for low impedance and high impedance respectively.

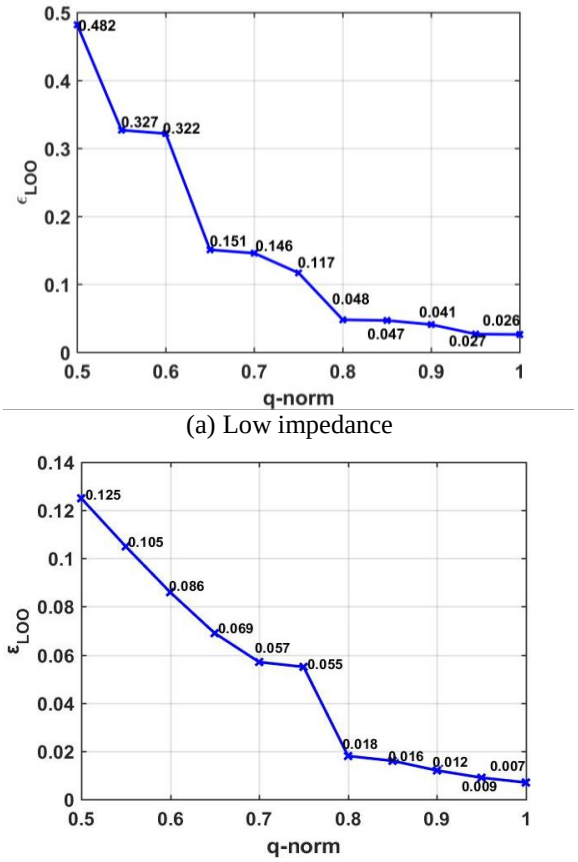

(a) Low impedance

(b) High impedance

Fig. 8. ε_{LOO} curve of different q norm.

Table 3: Comparison of sparse coefficient g with different q norm when P=15

q	0.5	0.55	0.6	0.65	0.7	0.75	0.8	0.85	0.9	0.95	1
N'	263	358	480	662	873	1133	1476	1893	2404	3095	3876
g	6.79%	9.24%	12.4%	17.1%	22.5%	29.2%	38.1%	48.8%	62.0%	79.9%	1

According to Fig. 8, when q = 0.8, ε_{LOO} reaches the threshold value, and when q >0.8, ε_{LOO} changes slightly. Combined with the sparse coefficient (g) in Table 3, compared with q >0.8, when ε_{LOO} is nearly the same, sparse coefficient q = 0.8 is the smallest, and the calculation cost is the lowest. Therefore, q = 0.8 satisfies the expectation of this work and can complete the initial sparse processing of polynomials. q is set to 0.8 for further analysis. After completing the selection of hyperbolic truncation norm q, the LAR introduced in the previous paper, that is, AS-PC, is combined for a more intensive sparse processing of the model. The previous study proved that under the traditional truncation scheme, P = 15 can achieve good accuracy. To verify that P = 15 can also achieve ideal accuracy when using the AS-PC, the induced current at 50, 80, and 100MHz is also selected as an example to compare the different truncation orders, as shown in Fig. 9.

Figure 9 indicates that when q = 0.8, compared with the calculation result of low-order truncation, the different of ε_{LOO} between P = 15 and P = 20 is small and basically consistent, indicating that the proposed model can achieve

the ideal precision when q = 0.8 and P = 15. Therefore we take the P=15 as the truncation order for the following study. To further verify the accuracy of AS-PC, the probability distribution of the radiated susceptibility induced current of the MTLs at the frequency points of 50, 80, and 100MHz is calculated. The probability distribution curve of the radiated susceptibility induced current of the MTLs is calculated by combining with AS-PC, as shown in Fig. 10.

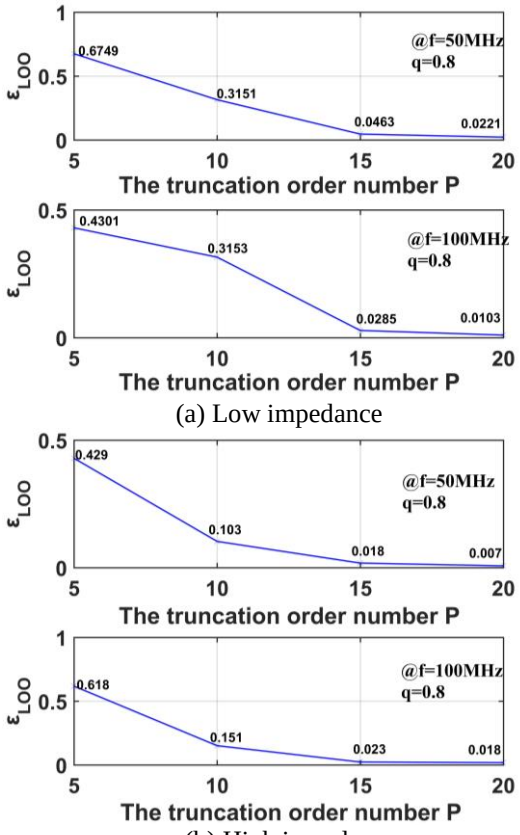

(a) Low impedance

(b) High impedance

Fig. 9. Comparison of different truncation order ε_{LOO} at different frequency points when q = 0.8 and P = 15.

The comparison of the results of the probability distribution curve in Fig. 10 shows that AS-PC can effectively calculate the probability distribution of induced current I_{R2} at different frequency points on the premise of ensuring the calculation accuracy, and we can see that in the case of low impedance, the induced current is smaller than that in the case of high impedance, which shows that increasing the load impedance of transmission line can effectively reduce the induced current when the transmission line is radiated. Take the case of low impedance, further analysis can be made by combining the calculation times of AS-PC and gPC and the sparse coefficient g, as shown in Table 4.

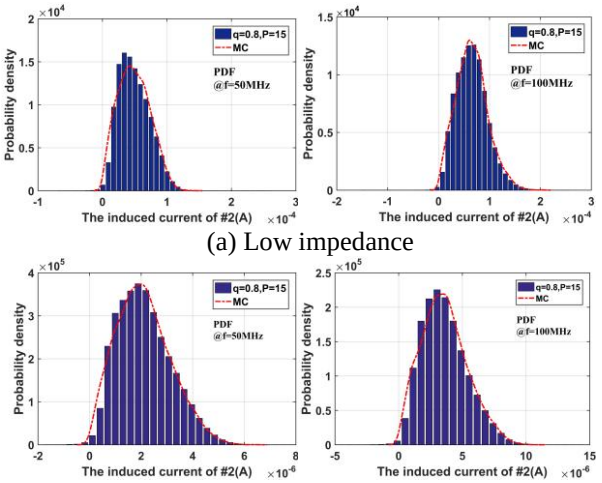

(a) Low impedance

(b) High impedance

Fig. 10. Comparison of induced current probability distribution of AS-PC calculated #2 transmission line at different frequency points.

Table 4: Computing time comparison between AS-PC and gPC

	Computing time (s)	g
AS-PC	6.39	3.25%
gPC	13.69	100%
20000 MC	2001.54	nan

The main frequency of the CPU used is 2.3GHz, and the RAM is 8GB. Table 4 shows that compared with the calculation time of 20000 MC realizations, the calculation time of gPC decreased greatly. However, AS-PC further compresses the calculation time effectively, saving calculation costs and improving the calculation efficiency while ensuring the calculation accuracy. On the basis of the above calculation results, AS-PC can effectively sparse gPC and accurately calculate the induced current probability distribution of the radiated susceptibility of MTLs at different frequency points.

The above calculation and analysis show that the AS-PC method can quickly and accurately calculate the relevant statistical characteristic parameters (such as the mean standard deviation probability distribution) in the uncertainties of the radiated susceptibility of MTLs on the premise of ensuring the calculation accuracy. Next, to further analyze the influence of different input variables on the model in the MTLs radiated susceptibility system, the global sensitivity calculation method introduced in the previous paper was studied.

The global sensitivity indices of each input variable are calculated by combining (10) and (11) and the expansion coefficients of AS-PC. Taking the response current at 50MHz at the right end of #2 transmission lines as an example, under different impedance conditions,

the total and first-order sensitivity indices of each input variable are calculated as follows.

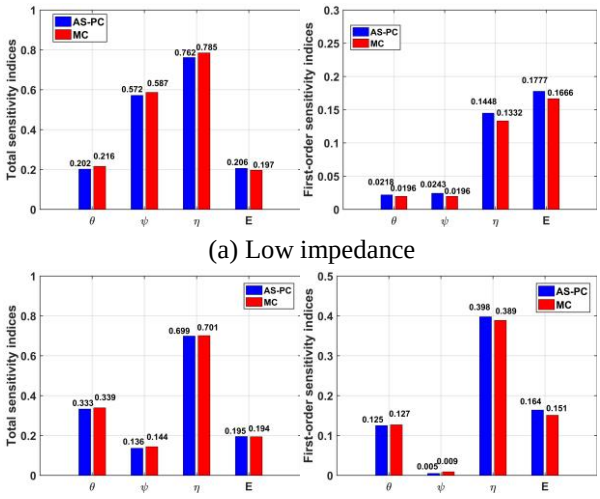

(a) Low impedance

(b) High impedance

Fig. 11. Comparison between the total and first-order sensitivity indices.

Figure 11 shows that the total and first-order sensitivity indices calculated based on the proposed method are basically the same as those calculated by the 20000 MC realizations, and the influence degree of various input variables on the model is also the same. The total sensitivity indices and the first-order sensitivity indices of the polarization angle η are both kept at a high level in the case of low impedance and high impedance, which is an important factor affecting the radiated susceptibility of the MTLs at this frequency point. However, in the case of low impedance, the sensitivity indices of elevation angle θ is low, which has little influence on the whole model. In the case of high impedance, the sensitivity indices of azimuth angle ψ is at a low level, which has less influence on the model than that of polarization angle η. On the basis of the above analysis, the proposed method is faster and more efficient and is thus effective in calculating the total sensitivity index and the first-order sensitivity indices of the radiated susceptibility of MTLs.

To more intuitively show the influence degree of different random variables at different frequency points on the whole model, the total sensitivity indices of the influence degree of each parameter on the radiated susceptibility of MTLs in the frequency band [10MHz, 1GHz] is calculated as shown in Fig. 12.

It can be seen from the analysis of Fig. 12 that no matter in the case of low impedance or high impedance, in the frequency band [10MHz, 1GHz], the influence degree of level amplitude E is maintained at a low level, which has little influence on the model as a whole. Although the influence is increased in the higher frequency band, such as [900MHz, 1GHz], the influence degree of polarization angle η at the same frequency band is far greater than level amplitude E, and when the frequency is higher than 200MHz, the influence degree of elevation angle θ on the model is also far greater. In the case of low impedance, azimuth ψ becomes an important factor affecting the model at about 200MHz, but the influence degree is greatly reduced at the high frequency, while in the case of high impedance, the influence of azimuth ψ is very weak at the low frequency. On the basis of the above analysis, when the location and frequency range of the radiation source in the surrounding environment are known in the practical engineering application, when designing the electrical system in this environment, attention should be paid to the polarization angle of the radiation source, and the position distribution of the transmission line should be adjusted reasonably and effectively to avoid unnecessary electromagnetic compatibility problems.

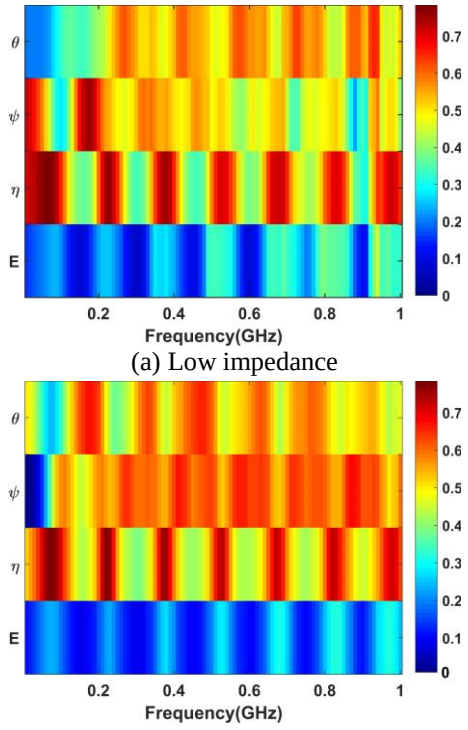

(a) Low impedance

(b) High impedance

Fig 12. [10MHz, 1GHz] influence of parameters on radiated susceptibility of MTLs.

IV. CONCLUSION

The uncertainties of the radiated susceptibility of MTLs with infinite ground as the reference conductor are studied. The elevation (θ), azimuth (ψ), polarization angle (η),and level amplitude (E) of the incident plane wave of the random input variables related to the radiated susceptibility of the MTLs are respectively subject to the

corresponding random distribution type. A surrogate model is established by gPC. On this basis, an AS-PC that combines the AHT with the LAR is proposed, and the gPC is sparsed and calculated to obtain the transmission lines-induced current (voltage)-related statistical information with different impedances, such as the mean value, the standard deviation, and the probability distribution. The comparison of the calculated results with 20000 MC realizations shows that the proposed method can effectively analyze the uncertainties of the radiated susceptibility of MTLs. Compared with the MC and gPC methods, AS-PC greatly improves the calculation efficiency and achieves fast calculation of the statistical characteristics of the radiated susceptibility of MTLs. Combined with the Sobol global sensitivity analysis method, the total and first-order sensitivity indices of the related random input variables in the radiated susceptibility model of MTLs are calculated, and the calculation results are compared with those of 20000 MC realizations. The comparison result proves that the proposed method can effectively calculate the influence degree of relevant parameters on the radiated susceptibility model of transmission lines. Therefore, the uncertainty analysis method for the radiated susceptibility of MTLs adopted in this paper can be used as a theoretical basis and reference for EMC design and rectification of relevant system cables.

ACKNOWLEDGMENT

This work was supported in part by the National Natural Science Foundation of China under Grant 51707080, and in part by the Jilin Scientific and Technological Development Program under Grant 20180101032JC, Grant 20190103055JH and Grant 20190303097SF.

REFERENCES

[1] C. Taylor, R. Satterwhite and C. Harrison, "The response of a terminated two-wire transmission line excited by a nonuniform electromagnetic field," *IEEE Trans. Antennas Propagat*., vol. 13, no. 6, pp. 987-989, Nov. 1965.

[2] C. R. Paul, "Frequency response of multiconductor transmission lines illuminated by an electromagnetic field," *IEEE Trans. on Electromagn. Compat.*, vol. EMC-18, no. 4, pp. 183-190, Nov. 1976.

[3] C. R. Paul, *Analysis of Multiconductor Transmission Lines*, 2nd ed., New York, NY, USA: Wiley, 2008.

[4] Z. Fei, Y. Huang, J. Zhou, and C. Song, "Numerical analysis of a transmission line illuminated by a random plane-wave field using stochastic reduced order models," *IEEE Access*, vol. 5, pp. 8741-8751, 2017.

[5] D. Bellan and S. Pignari, "A probabilistic model for the response of an electrically short two-conductor transmission line driven by a random plane wave field," *IEEE Trans. on Electromagn. Compat.*, vol. 43, no. 2, pp. 130-139, May 2001.

[6] S. Pignari and D. Bellan, "Statistical characterization of multiconductor transmission lines illuminated by a random plane-wave field," *IEEE International Symposium on Electromagnetic Compatibility Symposium Record*, Washington, DC, vol. 2, pp. 605-609, 2000.

[7] M. Omid, Y. Kami, and M. Hayakawa, "Field coupling to nonuniform and uniform transmission lines," *IEEE Trans. on Electromagn. Compat.*, vol. 39, no. 3, pp. 201-211, Aug. 1997.

[8] G. S. Shinh, N. M. Nakhla, R. Achar, M. S. Nakhla, A. Dounavis, and I. Erdin, "Fast transient analysis of incident field coupling to multiconductor transmission lines," *IEEE Trans. on Electromagn. Compat.*, vol. 48, no. 1, pp. 57-73, Feb. 2006.

[9] X. Zhang, Z. Zhao, Y. Qin, J. Luo, and G. Ni, "Transient analytic solutions of lossless multiconductor transmission line excited by plane-wave," *Proceedings of the 9th International Symposium on Antennas, Propagation and EM Theory*, Guangzhou, pp. 1073-1076, 2010.

[10] B. Ravelo, Y. Liu, and A. K. Jastrzebski, "PCB near-field transient emission time-domain model," *IEEE Trans. Electromagn. Compat.*, vol. 57, no. 6, pp. 1320-1328, Dec. 2015.

[11] L. Gao, Q. Yu, D. Wu, T. Wang, X. Yu, Y. Chi, and T. Zhang, "Probabilistic distribution modeling of crosstalk in multi-conductor transmission lines via maximum entropy method," in *IEEE Access*, vol. 7, pp. 103650-103661, 2019.

[12] Y. Chi, B. Li, X. Yang, T. Wang. K. Yang, and Y. Gao, "Research on the statistical characteristics of crosstalk in naval ships wiring harness based on polynomial chaos expansion method," *Nephron. Clin. Pract*., vol. 24, no. s2, pp. 205-214, 2017.

[13] P. Manfredi and F. G. Canavero, "Polynomial chaos representation of transmission-line response to random plane waves," *International Symposium on Electromagnetic Compatibility - EMC Europe*, Rome, pp. 1-6, 2012.

[14] P. Manfredi and F. G. Canavero, "Polynomial Chaos for Random Field Coupling to Transmission Lines," in *IEEE Trans. Electromagn. Compat.*, vol. 54, no. 3, pp. 677-680, June 2012.

[15] T. Bdour and A. Reineix, "Global sensitivity analysis and uncertainty quantification of radiated susceptibility in PCB using nonintrusive polynomial chaos expansions," *IEEE Trans. Electromagn. Compat.*, vol. 58. no. 3, pp. 939-942, June 2016.

[16] B. Efron, T. Hastie, I. Johnstone, and R. Tibshirani, "Least angle regression," *The Annals of Statistics*, vol. 32, no. 2, pp. 407-451, 2004.

[17] G. Blatman and B. Sudret, "Adaptive sparse

polynomial chaos expansion based on least angle regression," *J. Comput. Phys.*, vol. 230, no. 6, pp. 2345-2367, Dec. 2011.

[18] G. Spadacini, F. Grassi, F. Marliani, and S. A. Pignari, "Transmission-line model for field-to-wire coupling in bundles of twisted-wire pairs above ground," *IEEE Trans. Electromagn. Compat.*, vol. 56, no. 6, pp. 1682-1690, Dec. 2014.

[19] G. Spadacini and S. A. Pignari, "Numerical assessment of radiated susceptibility of twisted-wire pairs with random nonuniform twisting," *IEEE Trans. Electromagn. Compat.*, vol. 55, no. 5, pp. 956-964, Oct. 2013.

[20] H. Y. Xie, Y. Li, and H. L. Qiao, "Analysis of field coupling to transmission lines with random rotation over the ground," *Chin. Phys. B.*, vol. 24, no. 6, pp. 171-176, Apr. 2015.

[21] I. M. Sobol, "Global sensitivity indices for nonlinear mathematical models and their Monte Carlo estimates," *Math. Comput. Simul.*, vol. 55, no. 1-3, pp. 271-280, 2001.

[22] A. Kouassi, J. Bourinet, S. Lalléchère, P. Bonnet, and M. Fogli, "Reliability and sensitivity analysis of transmission lines in a probabilistic EMC context," *IEEE Trans. Electromagn. Compat.*, vol. 58, no. 2, pp. 561-572, Apr. 2016.

[23] N. Wiener, "The homogeneous chaos," *Am. J. Math*., vol. 60, pp. 897-936, 1938.

[24] N. Wiener, *Nonlinear Problems in Random Theory*. MIT Technology Press and John Wiley and Sons, 1958.

[25] D. Xiu and G. E. Karniadakis, "Modeling uncertainty in flow simulations via generalized polynomial chaos," *J. Comput. Phys.*, vol. 187, no. 1, pp. 137-167, 2003.

[26] R. Mukerjee and C. F. J. Wu, *A Modern Theory of Factorial Designs*. *Springer New York*, 2006.

[27] M. Larbi, I. S. Stievano, F. G. Canavero, and P. Besnier, "Identification of main factors of uncertainty in a microstrip line network," *Prog. Electromagn. Res*., vol. 162, pp. 61-72, 2018.

[28] B. Sudret, "Global sensitivity analysis using polynomial chaos expansions," *Reliability Engineering and System Safety*, vol. 93, no. 7, pp. 964-979, Apr. 2008.